Article

Cell Reports

RACK1 Promotes Autophagy by Enhancing the Atg14L-Beclin 1-Vps34-Vps15 Complex Formation upon Phosphorylation by AMPK

Graphical Abstract

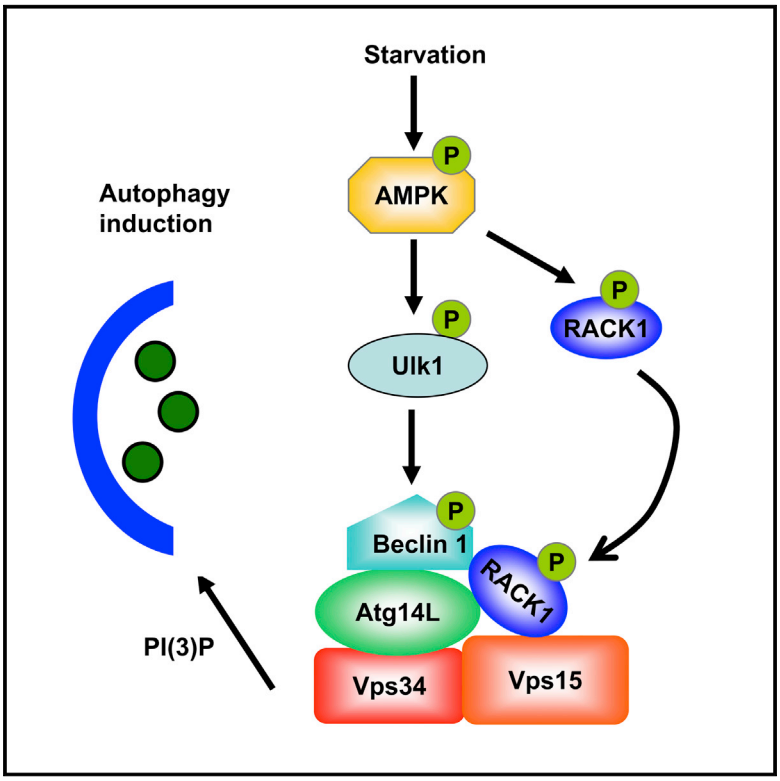

Authors

Yawei Zhao, Qingyang Wang, Guihua Qiu, ..., Weiping J. Zhang, Yuanfang Ma, Jiyan Zhang

Correspondence

zhangjy@nic.bmi.ac.cn

In Brief

Adaptors have emerged as key factors in autophagy onset with elusive recruitment mechanism(s). Here, Zhao et al. demonstrate that RACK1, upon phosphorylation by AMPK, works as an adaptor essential for the assembly of the Atg14L-Beclin 1-Vps34-Vps15 complex. RACK1 deficiency in hepatocytes leads to lipid accumulation in the liver.

Highlights

- Hepatocyte-specific RACK1 deficiency leads to lipid accumulation in the liver
- RACK1 deficiency results in defective autophagy onset
- RACK1 participates in the formation of autophagosome biogenesis complex
- RACK1 promotes autophagy upon its phosphorylation by AMPK

Zhao et al., 2015, Cell Reports *13*, 1407–1417
November 17, 2015 ©2015 The Authors
http://dx.doi.org/10.1016/j.celrep.2015.10.011

Cell Reports
Article

RACK1 Promotes Autophagy by Enhancing the Atg14L-Beclin 1-Vps34-Vps15 Complex Formation upon Phosphorylation by AMPK

Yawei Zhao,[1,2,5] Qingyang Wang,[1,5] Guihua Qiu,[1] Silei Zhou,[1,2] Zhaofei Jing,[1] Jingyang Wang,[1] Wendie Wang,[1,2] Junxia Cao,[1] Kun Han,[1] Qianqian Cheng,[1] Beifen Shen,[1] Yingyu Chen,[3] Weiping J. Zhang,[4] Yuanfang Ma,[2] and Jiyan Zhang[1,*]

[1]Department of Molecular Immunology, Institute of Basic Medical Sciences, 27 Taiping Road, Beijing 100850, PRC
[2]Key Laboratory of Cellular and Molecular Immunology, Henan University, Kaifeng, Henan 475001, PRC
[3]Key Laboratory of Medical Immunology, Ministry of Health, Peking University Health Science Center, Beijing 100083, PRC
[4]Department of Pathophysiology, Second Military Medical University, 800 Xiangyin Road, Shanghai 200433, PRC
[5]Co-first author
*Correspondence: zhangjy@nic.bmi.ac.cn
http://dx.doi.org/10.1016/j.celrep.2015.10.011

SUMMARY

Autophagy is essential for maintaining tissue homeostasis. Although adaptors have been demonstrated to facilitate the assembly of the Atg14L-Beclin 1-Vps34-Vps15 complex, which functions in autophagosome formation, it remains unknown whether the autophagy machinery actively recruits such adaptors. WD40-repeat proteins are a large, highly conserved family of adaptors implicated in various cellular activities. However, the role of WD40-repeat-only proteins, such as RACK1, in postnatal mammalian physiology remains unknown. Here, we report that hepatocyte-specific RACK1 deficiency leads to lipid accumulation in the liver, accompanied by impaired Atg14L-linked Vps34 activity and autophagy. Further exploration indicates that RACK1 participates in the formation of autophagosome biogenesis complex upon its phosphorylation by AMPK at Thr50. Thr50 phosphorylation of RACK1 enhances its direct binding to Vps15, Atg14L, and Beclin 1, thereby promoting the assembly of the autophagy-initiation complex. These observations provide insight into autophagy induction and establish a pivotal role for RACK1 in postnatal mammalian physiology.

INTRODUCTION

Autophagy is a conserved eukaryotic process that degrades long-lived proteins and other cytoplasmic contents such as aggregated proteins, damaged/excess organelles, and lipids through lysosomes (Kim and Lee, 2014; Kraft and Martens, 2012; Mizushima and Komatsu, 2011). Although autophagy usually occurs in response to starvation and other stresses, this process also happens under nutrient-rich conditions (basal or constitutive autophagy) (Hara et al., 2006; Komatsu et al., 2005; Nakai et al., 2007; Takamura et al., 2011). Hepatocytes exhibit significant levels of basal autophagy, which makes the liver a convenient organ for examining autophagic regulation (Komatsu et al., 2005; Takamura et al., 2011). Hepatocytes are a major cellular storehouse for neutral lipids in the form of triglycerides (TGs) and cholesterol esters contained in specialized organelles termed "lipid droplets." Studies have now clearly demonstrated that autophagy mediates the breakdown of intracellular stores of lipid droplets (Singh et al., 2009). The loss of hepatocyte autophagy leads to a marked increase in liver TG and cholesterol content, demonstrating that autophagy limits hepatocyte lipid accumulation in vivo (Jaber et al., 2012; Komatsu et al., 2005; Singh et al., 2009; Takamura et al., 2011).

Vps34, which converts phosphatidylinositol (PtdIns) to PtdIns 3-phosphate (PI(3)P), is the only class III PtdIns 3-kinase (PI3K) in mammals. By forming a stable complex with a putative Ser-Thr protein kinase, Vps15, Vps34 lipid kinase behaves as a key regulator of autophagy initiation and progression (Liang et al., 2006; Matsunaga et al., 2009). At the different stages of autophagy, different complexes containing Vps34-Vps15 form and exert distinct functions. The Atg14L-Beclin 1-Vps34-Vps15 complex functions in autophagosome formation, the UVRAG-Beclin 1-Vps34-Vps15 complex functions in autophagosome and endosome maturation, and the Rubicon-UVRAG-Beclin 1-Vps34-Vps15 complex is thought to suppress autophagosome and endosome maturation (Liang et al., 2006; Matsunaga et al., 2009). The assembly of the autophagy-initiation complex depends on Beclin 1 phosphorylation by Ulk1 (Russell et al., 2013). AMP-activated protein kinase (AMPK), a key energy sensor activated by nutrient deprivation, directly activates Ulk1 through phosphorylation at several serines, including Ser555 (Egan et al., 2011; Kim et al., 2011). By contrast, high activity of mammalian target of rapamycin (mTOR) under nutrient-rich conditions prevents Ulk1 activation by phosphorylating Ulk1 Ser757 and disrupting the interaction between Ulk1 and AMPK (Kim et al., 2011). Moreover, Bcl-2 dissociation from Beclin 1 triggered by JNK-mediated Bcl-2 phosphorylation promotes

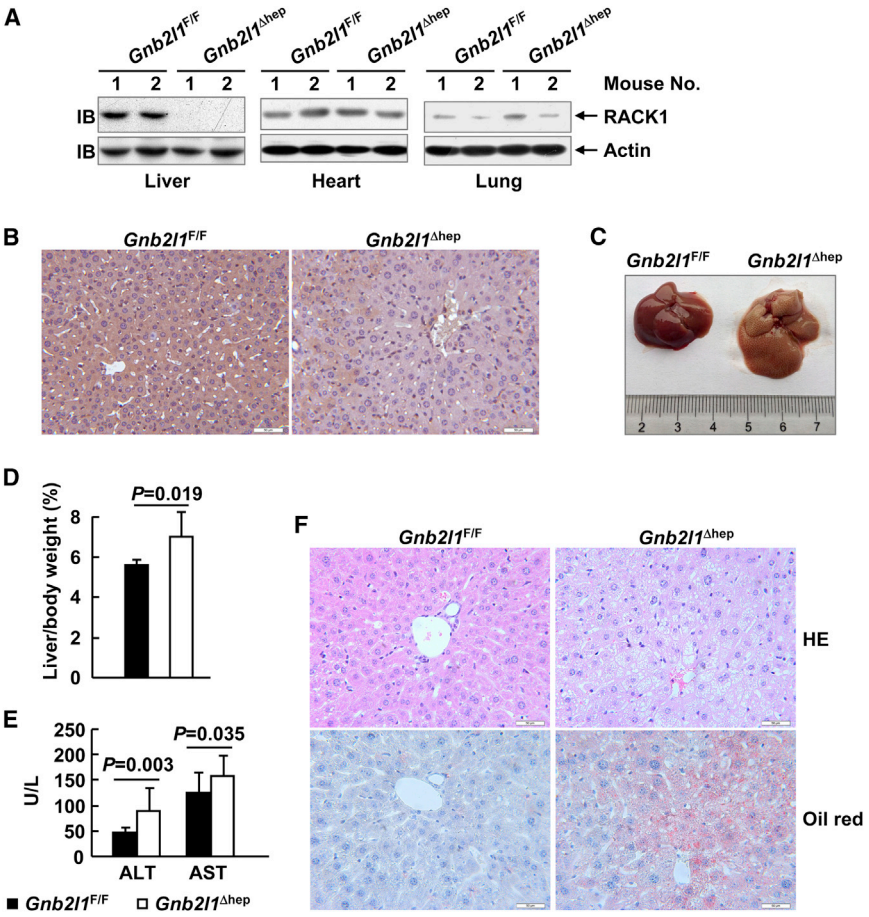

Figure 1. Hepatocyte-Specific RACK1 Deficiency Leads to Hepatosteatosis

(A) IB analysis of RACK1 expression in the indicated tissues of 6-week-old *Gnb2l1*$^{F/F}$ and *Gnb2l1*$^{\Delta hep}$ mice.

(B) Immunohistochemistry for RACK1 expression in liver sections of 6-week-old *Gnb2l1*$^{F/F}$ and *Gnb2l1*$^{\Delta hep}$ mice. Scale bars, 50 μm.

(C) Representative image of livers from 4-month-old *Gnb2l1*$^{F/F}$ and *Gnb2l1*$^{\Delta hep}$ mice.

(D) Liver weight relative to body weight for 4-month-old *Gnb2l1*$^{F/F}$ and *Gnb2l1*$^{\Delta hep}$ mice (n = 6).

(E) Serum levels of ALT and AST in 4-month-old *Gnb2l1*$^{F/F}$ (n = 13) and *Gnb2l1*$^{\Delta hep}$ (n = 25) mice. U/L, units per liter.

(F) H&E (HE) staining (top) and oil red staining (bottom) of liver sections from 4-month-old *Gnb2l1*$^{F/F}$ and *Gnb2l1*$^{\Delta hep}$ mice. Scale bar, 50 μm.

Error bars indicate mean ± SD.

Atg14L-Beclin 1-Vps34-Vps15 complex formation (Wei et al., 2008). Recently, emerging evidence suggests that certain scaffold proteins contribute to the formation of the autophagy-initiation complex as binding partners (Araki et al., 2013; Lu et al., 2014; Ma et al., 2014). However, it remains unknown whether the autophagy machinery actively recruits adaptors or not.

WD40 repeats are ~40-amino-acid motifs, usually ending with a Trp-Asp (W-D) dipeptide (Stirnimann et al., 2010). WD40-repeat proteins are a large family highly conserved in all eukaryotes and are implicated in a variety of functions, including cell cycle control and apoptosis (Liu et al., 2007; Stirnimann et al., 2010). Despite that, the in vivo functions of WD40 repeats have been studied less intensely than other common domains like the kinase, PDZ, or SH3 domains (Stirnimann et al., 2010). To date, the role of WD40-repeat-only proteins in postnatal mammalian physiology remains unknown. Receptor for activated C kinase 1 (RACK1, official gene name *Gnb2l1*) was originally identified on the basis of its ability to anchor activated form of protein kinase C (PKC). As a WD40-repeat-only protein, it has been recognized as an adaptor protein involved in multiple intracellular signaling pathways. While ubiquitously distributed in the tissues of mammals, RACK1 is highly expressed in normal liver (Guo et al., 2013; Ruan et al., 2012). Thus, it is of interest to disclose how RACK1 functions in liver physiology. Here, we report that RACK1, upon Thr50 phosphorylation by AMPK, works as an adaptor essential for the assembly of the Atg14L-Beclin 1-Vps34-Vps15 complex. RACK1 deficiency in hepatocytes leads to lipid accumulation in the liver.

RESULTS

Hepatocyte-Specific RACK1 Deficiency Leads to Hepatosteatosis

To study the role of RACK1 in liver physiology, we generated a liver-specific conditional knockout mouse model for RACK1. We used the *Cre-loxP* system to conditionally disrupt the 172-bp region in exon 2 of the *gnb2l1* gene. Crossing mice carrying the floxed *gnb2l1* allele (*Gnb2l1*$^{F/F}$) with mice expressing Cre recombinase under the control of the *albumin* promoter and enhancer (Postic et al., 1999) allowed us to generate a liver-specific RACK1 knockout mouse model (*Alb-Cre*:*Gnb2l1*$^{F/F}$; hereinafter referred to as *Gnb2l1*$^{\Delta hep}$; Figure S1A). *Gnb2l1*$^{\Delta hep}$ mice were born at Mendelian frequency and proportional male/female ratios (data not shown). Genotyping confirmed the presence of *LoxP* sites and *Alb-Cre* in *Gnb2l1*$^{\Delta hep}$ mice (Figure S1B). Immunoblotting (IB) and immunohistochemistry analysis revealed that the levels of RACK1 protein were almost undetectable in livers of *Gnb2l1*$^{\Delta hep}$ mice when compared with those of *Gnb2l1*$^{F/F}$ mice (Figures 1A and 1B). However, levels of RACK1 were unaltered in other tissues (Figure 1A; data not shown). The livers of *Gnb2l1*$^{\Delta hep}$ mice looked normal in the first 12 weeks of life (data not shown). After that, *Gnb2l1*$^{\Delta hep}$ mice began to show enlarged and discolored livers, which weighed more than those from *Gnb2l1*$^{F/F}$ mice (Figures 1C and 1D). *Gnb2l1*$^{\Delta hep}$ mice exhibited discrete but significantly elevated serum alanine aminotransferase (ALT) and aspartate transaminase (AST), markers of hepatocyte damage (Figure 1E) as early as 4 months of age. Consistently, hepatocytes from *Gnb2l1*$^{\Delta hep}$ mice contained

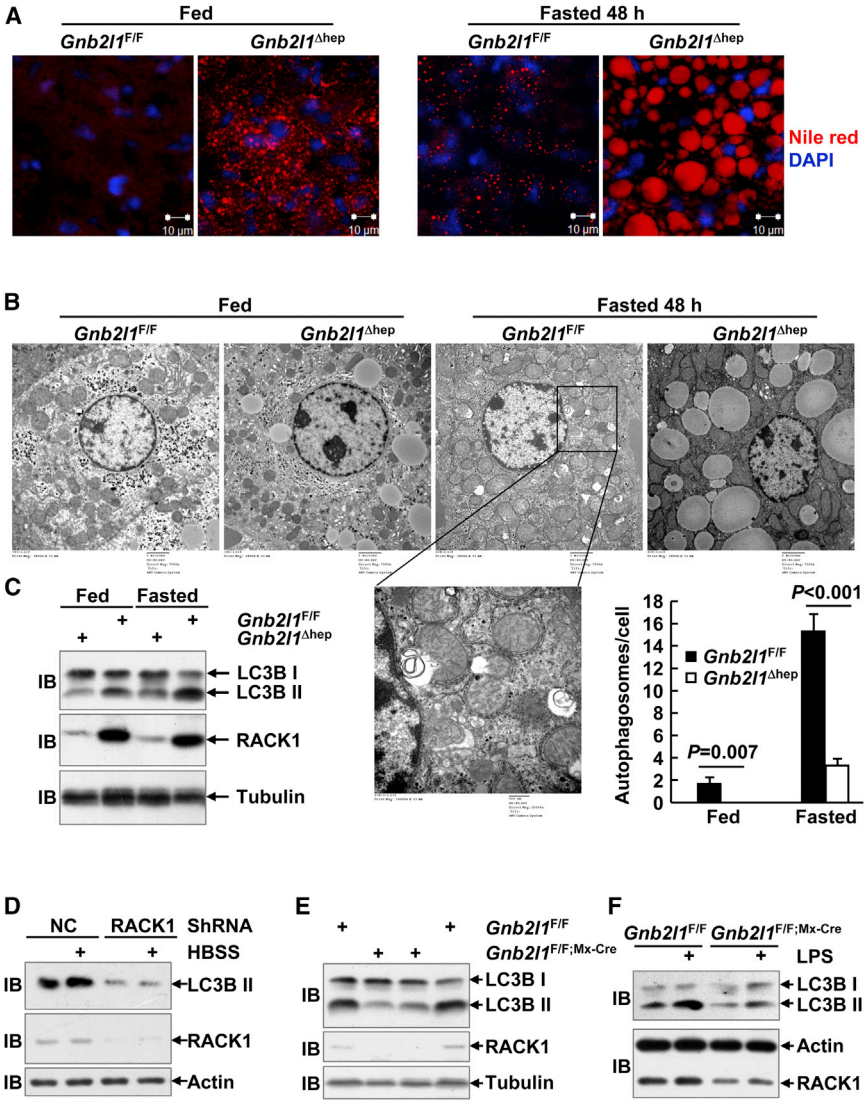

Figure 2. RACK1 Is Involved in Autophagy

(A–C) Nile red staining (A; scale bar, 10 μm), electron microscopy (B; scale bar, 2 μm or 500 nm), or IB analysis (C) of liver sections from fed and 48-hr-fasted 6-week-old mice with the indicated genotypes.

(D–F) HepG2 cells stably expressing RACK1 shRNA or non-targeting control (NC) shRNA were cultured in Hank's balanced salt solution (HBSS) for 4 hr or left untreated (D); heart tissues were harvested from *Gnb2l1*$^{F/F}$ and *Gnb2l1*$^{F/F;Mx\text{-}Cre}$ mice 8 weeks after poly(I:C) injections (E); or peritoneal macrophages from *Gnb2l1*$^{F/F}$ and *Gnb2l1*$^{F/F;Mx\text{-}Cre}$ mice 8 weeks after poly(I:C) injections were treated with or without 1 μg/ml LPS for 24 hr (F). LC3B-II levels were then analyzed by IB. Note that LC3B-I was not detected in HepG2 cells.

round cytosolic structures (Figure 1F) that stained positive with the neutral lipid dye oil red O (Figure 1F). The liver damage associated with lipid accumulation in *Gnb2l1*$^{\Delta hep}$ mice eventually leads to spontaneous tumors (Figures S1C and S1D). Tumors were generated in all the *Gnb2l1*$^{\Delta hep}$ mice examined (5/5) at the age of 19 months, and three out of five *Gnb2l1*$^{\Delta hep}$ mice developed tumors bigger than 5 mm (Figures S1C and S1D).

RACK1 Is Involved in Autophagy

To further explore the physiological role of RACK1 in the liver, 6-week-old *Gnb2l1*$^{\Delta hep}$ mice and their littermates were subjected to fasting, which causes mobilization of lipids from peripheral depots into the liver (McCue 2010; Zoncu et al., 2011). Lipid staining with Nile red revealed increased lipid storage in fed *Gnb2l1*$^{\Delta hep}$ livers, which became even more evident after starvation (Figure 2A). The giant neutral lipid structures in fasted *Gnb2l1*$^{\Delta hep}$ livers shown in Figure 2A might result from the fusion of big and closely located lipid droplets during Nile red staining.

Ultrastructural analysis confirmed an increased number of cytosolic lipid droplets in fed *Gnb2l1*$^{\Delta hep}$ livers (Figure 2B). Furthermore, smaller mitochondria and the lack of glycogen deposition were also observed in fed *Gnb2l1*$^{\Delta hep}$ livers (Figure 2B). Notably, although a 48-hr fasting induced autophagosomes in *Gnb2l1*$^{F/F}$ livers, *Gnb2l1*$^{\Delta hep}$ livers exhibited virtually no autophagosomes, lipid droplets with increased number and size, and many swollen mitochondria (Figure 2B). These phenotypes are consistent with those observed in autophagy-deficient Vps34$^{-/-}$ livers (Jaber et al., 2012). Indeed, IB analysis revealed that *Gnb2l1*$^{\Delta hep}$ livers showed diminished basal and starvation-induced membrane-bound LC3B-II generation from cytosolic LC3B-I (Figure 2C), an indicator of autophagic acitivity. Consistently, indirect immunofluorescence (IF) analysis of endogenous LC3B demonstrated that primary hepatocytes purified from *Gnb2l1*$^{\Delta hep}$ mice exhibited reduced numbers of LC3B-positive dots (autophagic LC3 puncta), both at the basal state and after rapamycin treatment (Figure S2A). In addition, short hairpin RNA (shRNA)-mediated stable knockdown of RACK1 in HepG2 human hepatoma cells or BNL CL.2 normal murine hepatocytes significantly suppressed basal levels of LC3B-II formation as well as LC3B-II conversion in response to nutrient deprivation (Figure 2D), rapamycin (Figure S2B), or endoplasmic reticulum (ER) stress-inducer tunicamycin (TN) (Figure S2C). In line with the lipid accumulation in *Gnb2l1*$^{\Delta hep}$ livers, Nile red staining revealed that RACK1 knockdown led to increased lipid storage in BNL CL.2 cells (Figure S2D).

To analyze whether RACK1 also promotes autophagy in tissues other than the liver, we crossed *Gnb2l1*$^{F/F}$ mice with mice expressing Cre recombinase downstream of the α/β-interferon-inducible Mx promoter. Cre recombinase activity was

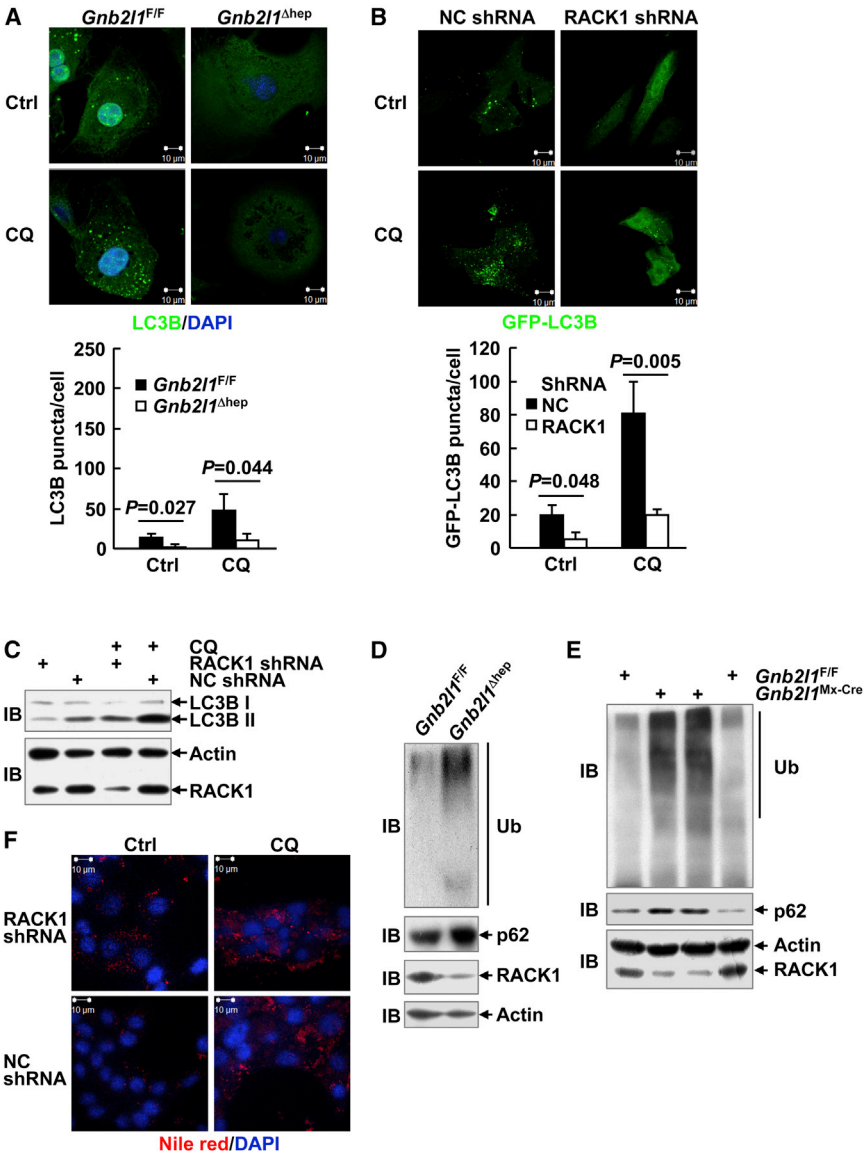

Figure 3. Autophagy Onset Is Impaired upon RACK1 Deficiency

(A) Indirect IF analysis (scale bar, 10 μm) of endogenous LC3B in primary hepatocytes treated with or without CQ (10 μM, 24 hr). Note that primary hepatocytes were isolated from 6-week-old mice with the indicated genotypes. Ctrl, control.

(B) HepG2 cells stably expressing RACK1 shRNA or NC shRNA were transfected with a mammalian expression vector encoding GFP-LC3B. After treatment with or without CQ (10 μM, 24 hr), cells were subjected to confocal microscopy. Scale bar, 10 μm.

(C) BNL CL.2 cells stably expressing RACK1 shRNA or NC shRNA were treated with CQ (10 μM, 24 hr) or left untreated. LC3B-II levels were then analyzed by IB.

(D and E) IB analysis of liver tissues of 4-month-old mice with the indicated genotypes (D) or heart tissues from *Gnb2l1*$^{F/F}$ and *Gnb2l1*$^{F/F;Mx\text{-}Cre}$ mice 8 weeks after poly(I:C) injections (E) with the indicated antibodies. Ub, ubiquitin.

(F) BNL CL.2 cells stably expressing RACK1 shRNA or NC shRNA were treated with CQ (10 μM, 72 hr) or left untreated. Lipid accumulation was analyzed by Nile red staining. Scale bar, 10 μm.

initiated by intraperitoneal injection of *Gnb2l1*$^{F/F;Mx\text{-}Cre}$ mice and their littermates with poly(I:C), which induces α/β interferon production. Typically, we analyzed these mice 8 weeks after inducing recombination to reduce any potential effects of the poly(I:C). IB analysis confirmed that the levels of RACK1 protein were almost undetectable in heart tissues of *Gnb2l1*$^{F/F;Mx\text{-}Cre}$ mice (Figure 2E). As expected, RACK1 deficiency led to reduced basal levels of LC3B-II formation in heart tissues (Figure 2E). Similarly, peritoneal macrophages isolated from *Gnb2l1*$^{F/F;Mx\text{-}Cre}$ mice showed reduced levels of RACK1 protein and reduced basal levels of LC3B-II formation, as well as LC3B-II conversion in response to a major component of the outer membrane of all Gram-negative bacteria—lipopolysaccharide (LPS)—as compared to those isolated from *Gnb2l1*$^{F/F}$ mice (Figure 2F). Consistent with the previous reports that depletion of autophagic proteins enhances endotoxin-induced interleukin (IL)-1β production (Nakahira et al., 2011; Saitoh et al., 2008), RACK1 deficiency resulted in augmented secretion of IL-1β from peritoneal macrophages at the basal state and in response to LPS (Figure S2E).

Autophagy Onset Is Impaired upon RACK1 Deficiency

Reduced LC3B-II levels result from either decreased autophagy onset or increased autophagic protein degradation. The increased lipid storage in *Gnb2l1*$^{\Delta hep}$ livers suggests that autophagy flux is blocked. To further address this issue, primary hepatocytes were purified from *Gnb2l1*$^{F/F}$ and *Gnb2l1*$^{\Delta hep}$ mice and were treated with lysosomal protease inhibitor chloroquine (CQ). Indirect IF analysis of endogenous LC3B revealed that CQ treatment led to increased numbers of LC3B puncta in control hepatocytes (Figure 3A), indicating an autophagic flux. However, LC3B-positive structures remained rare in RACK1-deficienct hepatocytes, even after CQ treatment (Figure 3A). Similarly, RACK1 knockdown in HepG2 or BNL CL.2 cells hindered the formation of punctuate GFP-LC3B structures (Figure 3B, as revealed by confocal microscopy) and endogenous LC3B II (Figures S3A and 3C, as revealed by IB analysis), both in the absence and in the presence of CQ. In addition, RACK1 knockdown in HepG2 cells led to reduced ability to process DQ-BSA (a derivative of BSA that generates a highly fluorescent product that can be monitored by flow cytometry after enzymatic cleavage in acidic intracellular lysosomal compartments) at the basal state and upon nutrient deprivation (Figure S3B). These data support a role

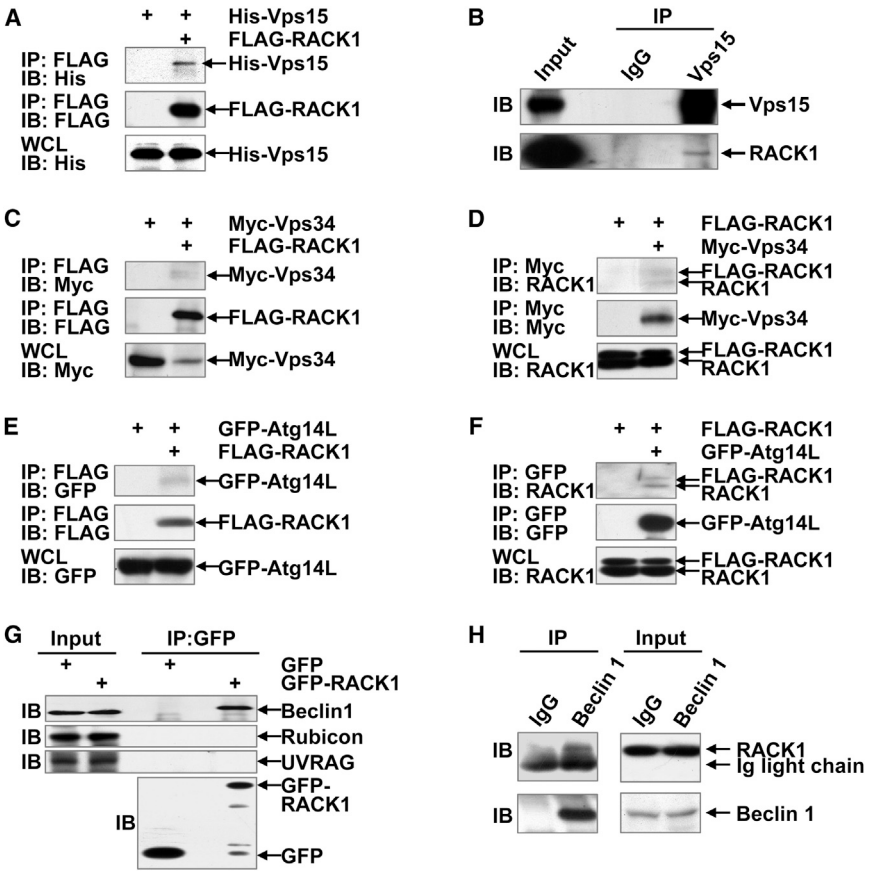

Figure 4. RACK1 Is a Component of the Atg14L-Beclin 1-Vps34-Vps15 Complex

(A and C–F) HepG2 cells were transfected with various mammalian expression vectors as indicated. Cell lysates were subjected to IP with the indicated antibodies. Precipitates were then subjected to SDS-PAGE and IB with the indicated antibodies. WCL, whole-cell lysates.

(B and H) IB analysis of the interaction between endogenous RACK1 and endogenous Vps15 or Beclin 1 in lysates of HepG2 cells after IP with an antibody against Vps15 or Beclin 1. Control antibody: rabbit immunoglobulin (Ig)G.

(G) HepG2 cells stably expressing both human RACK1 shRNA and GFP or GFP-tagged human RACK1 were subjected to IP with an antibody against GFP. Precipitates were then subjected to SDS-PAGE and IB with the indicated antibodies.

of RACK1 in autophagy onset. Impaired autophagy onset was associated with the accumulation of polyubiquitinated proteins and p62/Sqstm1 in *Gnb2l1*$^{\Delta hep}$ livers (Figure 3D) and *Gnb2l1*$^{F/F;Mx\text{-}Cre}$ hearts (Figure 3E).

To test whether impaired autophagic flux contributes to the increased lipid storage upon RACK1 deficiency, BNL CL.2 cells stably expressing RACK1 shRNA and control cells were treated with CQ. As expected, Nile red staining revealed that autophagy inhibition with CQ highly increased the accumulation of lipid droplets (Figure 3F). The differences between BNL CL.2 cells stably expressing RACK1 shRNA and control cells diminished following treatment with CQ (Figure 3F). These data indicate that inhibiting autophagy eliminates the deleterious roles of RACK1 knockdown, substantiating the finding that autophagy is required for RACK1-mediated protection against hepatic lipid accumulation.

RACK1 Is a Component of the Atg14L-Beclin 1-Vps34-Vps15 Complex

To explore how RACK1 is involved in autophagy onset, we generated HepG2 cells stably expressing both human RACK1 shRNA and GFP or GFP-tagged human RACK1 (HRshGFP-RACK1). Because GFP-RACK1 was also targeted by RACK1 shRNA, the total protein level of endogenous RACK1 and GFP-RACK1 in HRshGFP-RACK1 cells was still lower than the protein level of endogenous RACK1 in HepG2 cells stably expressing non-targeting control shRNA (Figure S4A). In this scenario, GFP-RACK1 should behave as endogenous RACK1 (thereafter referred to as endogenous-like GFP-RACK1) in HRshGFP-RACK1 cells. To examine RACK1-mediated protein-protein interaction upon autophagy induction, HRshGFP-RACK1 cells were subjected to nutrient deprivation or left untreated, followed by immunoprecipitation with an anti-GFP antibody covalently linked to sepharose beads. Silver staining compatible with mass spectrometry revealed that protein-protein interaction mediated by endogenous-like GFP-RACK1 was augmented upon starvation (Figure S4B). Eight specific bands were excised and subjected to mass spectrometry, which identified a fragment of Vps15 at the size of about 60–70 kDa (Figure S4B; Table S1). These data suggest that RACK1 may participate in autophagy induction as part of the autophagy-initiation complex. Indeed, co-immunoprecipitation (co-IP) analysis revealed the interaction of RACK1 with the autophagy-initiation complex in HepG2 cells: His-Vps15 co-precipitated with co-expressed FLAG-RACK1, and endogenous RACK1 co-precipitated with endogenous Vps15 (Figures 4A and 4B); Myc-Vps34 co-precipitated with co-expressed FLAG-RACK1, and FLAG-RACK1 co-precipitated with co-expressed Myc-Vps34 (Figures 4C and 4D); GFP-Atg14L co-precipitated with co-expressed FLAG-RACK1, and FLAG-RACK1 co-precipitated with co-expressed GFP-Atg14L (Figures 4E and 4F); endogenous Beclin 1 co-precipitated with endogenous-like GFP-RACK1, and endogenous RACK1 co-precipitated with endogenous Beclin 1 (Figures 4G and 4H). However, endogenous Rubicon and UVRAG were not detected in endogenous-like GFP-RACK1 precipitates under the same conditions (Figure 4G). Thus, it is unlikely that RACK1 affects the UVRAG-Beclin 1-Vps34-Vps15 complex or the Rubicon-UVRAG-Beclin 1-Vps34-Vps15 complex.

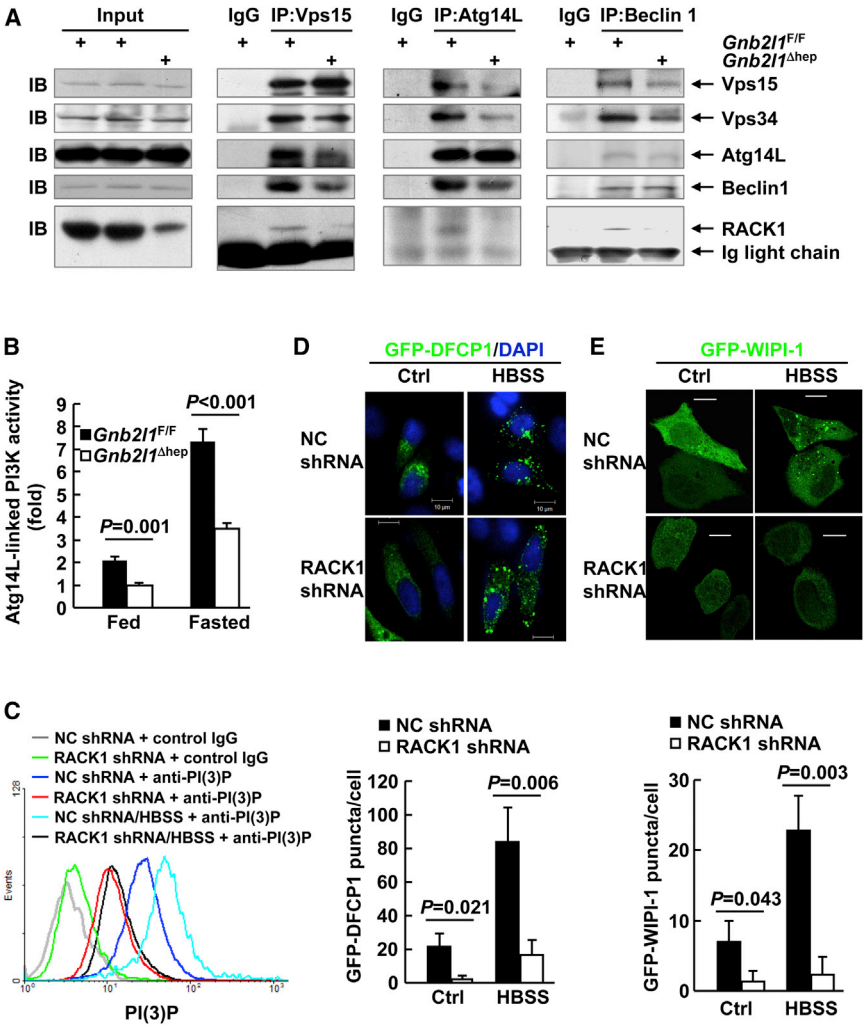

Figure 5. RACK1 Enhances the Assembly of the Autophagy-Initiation Complex

(A) Liver lysates from *Gnb2l1*$^{F/F}$ and *Gnb2l1*$^{\Delta hep}$ mice were subjected to IP with an antibody against Vps15, Atg14L, or Beclin 1. Precipitates were then subjected to SDS-PAGE and IB with the indicated antibodies. Control antibody: rabbit IgG.

(B) Endogenous Atg14L was immunoprecipitated from liver tissues of fed and 48-hr-fasted 6-week-old mice with the indicated genotypes, and Atg14L-linked Vps34 kinase activity was measured with the Class III PI3K ELISA Kit.

(C) Flow cytometry analysis of basal and nutrient-deprivation (HBSS, 4 hr)-induced PI(3)P generation in HepG2 cells stably expressing RACK1 shRNA or NC shRNA with an antibody against PI(3)P.

(D and E) Confocal microscopy (scale bar, 10 μm) of basal and nutrient deprivation (HBSS 4 h)-induced GFP-DFCP1 puncta (D) or GFP-WIPI-1 puncta (E) in HepG2 cells stably expressing RACK1 shRNA or NC shRNA. Ctrl, control.

RACK1 Enhances the Assembly of the Autophagy-Initiation Complex

Next, we tried to analyze whether RACK1 affects the formation of autophagy-initiation complex, particularly in tissues at the basal state. IB analysis revealed little change in the basal protein levels of Atg14L, Beclin 1, Vps34, and Vps15 between *Gnb2l1*$^{F/F}$ and *Gnb2l1*$^{\Delta hep}$ livers (Figure 5A). However, upon using anti-Vps15 antibody to pull down Vps15 protein complexes, we found that Vps15 bound slightly less Vps34 and markedly less Atg14L and Beclin 1 in *Gnb2l1*$^{\Delta hep}$ livers (Figure 5A). Similarly, we found that Atg14L bound slightly less Beclin 1 and markedly less Vps15 and Vps34 in *Gnb2l1*$^{\Delta hep}$ livers upon using anti-Atg14L antibody (Figure 5A), and Beclin 1 bound slightly less Atg14L and markedly less Vps15 and Vps34 in *Gnb2l1*$^{\Delta hep}$ livers upon using anti-Beclin 1 antibody (Figure 5A). In all these assays, RACK1 was detected in immunoprecipitates obtained from lysates of *Gnb2l1*$^{F/F}$ livers but not *Gnb2l1*$^{\Delta hep}$ livers (Figure 5A). Therefore, RACK1 is critical for the assembly of the autophagy-initiation complex in vivo. Consistently, *Gnb2l1*$^{\Delta hep}$ livers showed diminished Atg14L-linked Vps34 kinase activity at the basal state and after 48 hr fasting when we examined Vps34 kinase activity in anti-Atg14L immunoprecipitates with PtdIns as the substrate (Figure 5B). Moreover, indirect IF analysis followed by flow cytometry using an anti-PI(3)P antibody revealed that RACK1 knockdown resulted in decreased amount of PI(3)P in HepG2 cells at the basal state and upon nutrient deprivation (Figure 5C).

The accumulation of PI(3)P generates a platform to recruit PI(3)P-binding proteins. The PI(3)P-binding protein WIPI-1 is then recruited to such a platform (Itakura and Mizushima, 2010). Meanwhile, DFCP1 relocalizes from the ER/Golgi to subdomains of the ER called omegasomes in a PI(3)P-dependent manner upon autophagy induction (Axe et al., 2008). As expected, RACK1 knockdown in HepG2 cells led to diminished numbers of punctuate structures of both GFP-DFCP1 and GFP-WIPI-1 at the basal state and upon nutrient deprivation (Figures 5D and 5E). All together, the aforementioned data indicate that RACK1 promotes the autophagy-initiation complex formation and Atg14L-linked Vps34 activity.

Next, we explore whether RACK1 affects other units of the autophagy machinery. IB analysis revealed that *Gnb2l1*$^{\Delta hep}$ livers showed no reduced Ulk1 phosphorylation at Ser555 (P-Ulk1) and JNK phosphorylation at Thr183 and Tyr185 (P-JNK), which indicate the activity of Ulk1 and JNK, respectively, at basal state and after 48 hr fasting (Figure S5A). Thus, RACK1 promotes the autophagy-initiation complex formation without affecting the activation of Ulk1 and JNK. In addition, RACK1 knockdown did not hinder carbonyl cyanide *m*-chlorophenylhydrazone (CCCP)-induced mitophagy in HepG2 cells, as indicated by Tom20 degradation and the formation of punctuate GFP-LC3B structures (Figure S5B). Because this process bypasses the autophagy-initiation complex (Chu et al., 2007), the autophagy machinery downstream should not be significantly impaired.

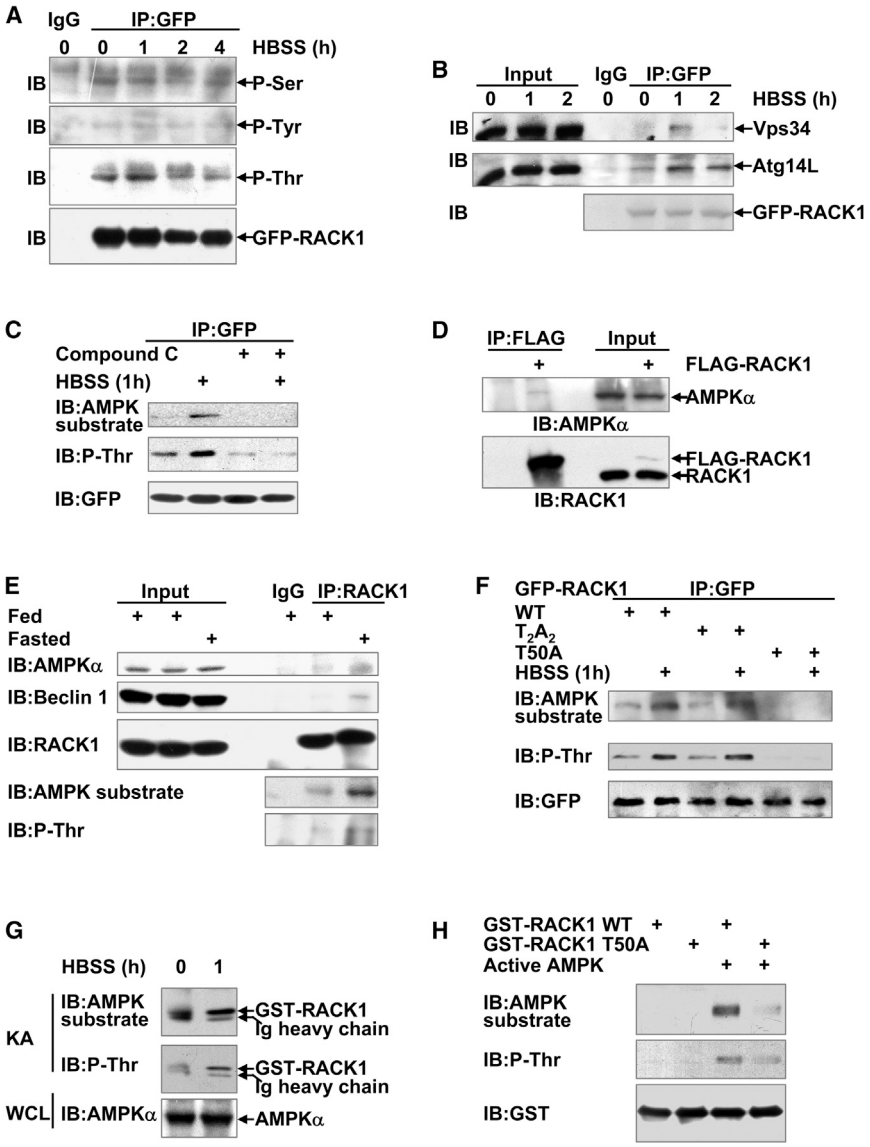

Figure 6. RACK1 Is Phosphorylated by AMPK at Thr50

(A–C) HepG2 cells stably expressing both human RACK1 shRNA and GFP-tagged human RACK1 were pretreated with or without compound C (10 μM, 1 hr). After culture in HBSS for various periods of time as indicated, cell lysates were subjected to IP with an anti-GFP antibody. Precipitates were then subjected to SDS-PAGE and IB with the indicated antibodies. Control antibody: rabbit IgG.

(D and E) HepG2 cells were transfected with or without a mammalian expression vector encoding FLAG-RACK1 (D), or liver tissues were prepared (E). Exogenous FLAG-RACK1 (D) or endogenous RACK1 (E) was immunoprecipitated with an antibody against FLAG or RACK1, respectively. Precipitates were then subjected to SDS-PAGE and IB with the indicated antibodies. Control antibody: rabbit IgG.

(F) HepG2 cells were transfected with mammalian expression vectors encoding GFP-tagged WT RACK1 or mutants. 24 hr later, cells were cultured in HBSS for 1 hr, and cell lysates were subjected to IP with an anti-GFP antibody. Precipitates were then subjected to SDS-PAGE and IB with the indicated antibodies.

(G and H) GST-RACK1 WT or GST-RACK1 T50A (2 μg each) was incubated with immunoprecipitated endogenous AMPK complex (G) or purified active AMPK complex (H) in AMPK kinase assay (KA) buffer. Nonradioactive ATP was added to drive the reaction. Samples were kept at 30°C for 20 min with gentle shaking. Then, 5% of the samples were subjected to SDS-PAGE and IB with the indicated antibodies. WCL, whole-cell lysates.

RACK1 Is Phosphorylated by AMPK at Thr50

Our work adds a member to the growing list of autophagy-initiation complex-binding partners. Then, what initiates the entry of RACK1 into this complex? We have noticed that, upon 48 hr fasting, RACK1 in livers could be occasionally detected as a doublet by IB (data not shown). Since RACK1 has been reported to undergo various phosphorylations (Belozerov et al., 2014; Chang et al., 2002; Kiely et al., 2009; Urano et al., 2015), it is possible that some type of RACK1 phosphorylation was enhanced upon autophagy induction. In this scenario, endogenous-like GFP-RACK1 was immunoprecipitated and subjected to IB. Our data revealed that endogenous-like GFP-RACK1 in HepG2 cells underwent various phosphorylations at the basal state (Figure 6A). However, only Thr phosphorylation of endogenous-like GFP-RACK1 in HepG2 cells was enhanced upon nutrient deprivation for 1 hr (Figure 6A). At this time point, the interaction between endogenous-like GFP-RACK1 with endogenous Vps34 and Atg14L was augmented (Figure 6B). Thus, it is possible that some Ser-Thr protein kinase phosphorylates RACK1, which initiates the entry of RACK1 into the autophagy-initiation complex.

To clarify the possible phosphorylation site(s) of RACK1 involved in autophagy onset, we immunoprecipitated endogenous-like GFP-RACK1 after nutrient deprivation for 1 hr and then carried out mass spectrometry analysis. Tandem mass spectrometry (MS/MS) analysis identified a phosphopeptide "DETNYGIPQR," with Thr50 as the phosphorylation site (Figure S6). The sequence surrounding Thr50 in human RACK1 is "LTRDET$_{50}$NYG," which matches the optimal AMPK substrate motif and is conserved in higher eukaryotes. In this scenario, we used compound C, a cell-permeable pyrazolopyrimidine compound that acts as a selective ATP-competitive inhibitor of AMPK (Bhutia et al., 2010). The result shows that compound C abolished basal and nutrient-deprivation-induced Thr phosphorylation of endogenous-like GFP-RACK1 (Figure 6C). IB analysis of the same precipitates with an antibody against phospho-AMPK substrate motif showed the same tendency (Figure 6C). The interaction of RACK1 with AMPKα, the catalytic subunit, was confirmed by co-IP analysis: endogenous AMPKα co-precipitated with both

exogenous FLAG-RACK1 in HepG2 cells (Figure 6D) and endogenous RACK1 in liver tissues (Figure 6E). The physiological interaction of AMPKα with RACK1 in liver tissues was augmented upon fasting (Figure 6E). Immunoprecipitated endogenous RACK1 in liver tissues was detected by antibodies against phospho-AMPK substrate motif and Thr phosphorylation at the basal state, which became more evident after 48 hr of fasting (Figure 6E). As expected, the key component of the autophagy initiation complex, Beclin 1, co-precipitated with endogenous RACK1 in liver tissues at the basal state, and the interaction was strengthened upon fasting (Figure 6E).

Then, Thr50 was replaced by nonphosphorylatable alanine (T50A) in the full-length GFP-tagged RACK1 using site-directed mutagenesis. We also included T197A/T199A mutation (T_2A_2) as control. Immunoprecipitated GFP-tagged wild-type (WT) RACK1 and T_2A_2 mutant, but not T50A mutant, were detected similarly by antibodies against phospho-AMPK substrate motif and Thr phosphorylation at the basal state and after induction by nutrient deprivation for 1 hr (Figure 6F). Immune complex kinase assays driven by nonradioactive ATP showed that nutrient-deprivation-activated AMPK significantly phosphorylated glutathione S-transferase (GST)-tagged RACK1, as revealed by IB analysis with antibodies against phospho-AMPK substrate motif and Thr phosphorylation (Figure 6G). We also carried out in vitro kinase assays driven by nonradioactive ATP. As shown in Figure 6H, GST-RACK1 WT incubated with purified active AMPK complex (α1β2γ2) was readily detected by antibodies against phospho-AMPK substrate motif and Thr phosphorylation, respectively (Figure 6H). However, GST-RACK1 T50A was barely detected by the two antibodies under the same conditions (Figure 6H). Collectively, our results strongly suggest that RACK1 is a substrate of AMPK and is phosphorylated at Thr50 by this kinase during autophagy onset.

Thr50 Phosphorylation of RACK1 Promotes Its Direct Binding to Vps15, Atg14L, and Beclin 1

Next, we set out to explore whether Thr50 phosphorylation of RACK1 promotes its entry into the autophagy-initiation complex. For this purpose, site-directed mutagenesis was introduced into mammalian expression vectors encoding GFP-tagged RACK1 WT and mutants to make them resistant to RACK1 shRNA. As expected, co-IP analysis revealed that significant amount of endogenous Atg14L, Beclin 1, Vps34, and Vps15 co-precipitated with exogenous RACK1 WT and T_2A_2 mutant, whereas these endogenous proteins barely co-precipitated with exogenous T50A mutant, in HepG2 cells with stable RACK1 knockdown (Figure 7A). Furthermore, ectopic expression of RACK1 WT and T_2A_2 mutant augmented the amount of endogenous Beclin 1, Vps34, and Vps15 that co-precipitated with endogenous Atg14L in HepG2 cells with stable RACK1 knockdown, which was associated with augmented levels of LC3B-II (Figure 7B). However, exogenous T50A mutant showed no such effect (Figure 7B).

In line with the aforementioned data, examination of Vps34 kinase activity in anti-Atg14L immunoprecipitates with PtdIns as the substrate revealed that ectopic expression of RACK1 WT and T_2A_2 mutant, but not T50A mutant, in HepG2 cells with stable RACK1 knockdown led to enhanced Atg-14L-linked Vps34 kinase activity at the basal state (Figure 7C), which was accompanied by increased punctuate structures of endogenous LC3B (Figure 7D). Moreover, ectopic expression of RACK1 T50E mutant, which mimics Thr50 phosphorylation, in HepG2 cells with stable RACK1 knockdown led to higher levels of LC3B-II than its WT counterpart (Figure 7E).

Then, how does RACK1 Thr50 phosphorylation promote the assembly of the autophagy-initiation complex? Since RACK1 is an adaptor and a component of the Atg14L-Beclin 1-Vps34-Vps15 complex, it is possible that Thr50 phosphorylation of RACK1 leads to some conformational changes that facilitate its direct binding to the key components of the autophagy-initiation complex. To test this idea, we performed in vitro GST pull-down assays to examine whether RACK1 directly interacts with these proteins. As expected, in-vitro-translated GFP-Atg14L, Beclin1, and His-Vps15, but not Myc-Vps34, were precipitated specifically by GST-RACK1, but not by GST alone (Figure S7). GST-RACK1 WT or GST-RACK1 T50A proteins were subjected to phosphorylation by active AMPK complex in the presence of nonradioactive ATP. As expected, GST-RACK1 T50A was phosphorylated to a much less extent to GST-RACK1 WT by active AMPK complex (Figure 7F). Then, GST-RACK1 proteins were isolated by Glutathione-Sepharose (GSH) beads and mixed with in-vitro-translated His-Vps15, Myc-Vps34, GFP-Atg14L, and Beclin 1. GST pull-down in combination with IB analysis revealed that phosphorylation by active AMPK complex augmented the binding of GST-RACK1 WT, but not GST-RACK1 T50A, to His-Vps15, GFP-Atg14L, and Beclin 1 (Figure 7F). Together, our data suggest that Thr50 phosphorylation of RACK1 promotes its direct binding to Vps15, Atg14L, and Beclin 1, thereby promoting the assembly of the autophagy-initiation complex.

DISCUSSION

Although a previous study has reported that RACK1 is involved in autophagosome formation in *Drosophila* (Erdi et al., 2012), it remains unknown whether it plays the same role in mammalian cells, and no mechanism has been provided. Here, we show that RACK1 promotes autophagy in several types of mammalian cells in vivo and ex vivo. Furthermore, we show that RACK1 promotes the autophagy-initiation complex formation.

Autophagy limits hepatocyte lipid accumulation (Jaber et al., 2012; Komatsu et al., 2005; Singh et al., 2009; Takamura et al., 2011). Our data suggest that RACK1 prevents increased lipid storage in hepatocytes through promoting autophagy. Lipid droplet-autophagosome interplay also play pivotal roles in other models, such as macrophages or enterocytes. Uncontrolled accumulation of cholesteryl esters due to defective autophagy results in macrophage-derived foam cell formation, which is the initial stage of atherosclerosis (Li and Glass, 2002; Razani et al., 2012). Enterocytes face massive and immediate lipid volumes coming from the intestinal lumen. Recent progress has demonstrated an essential role of autophagy in the regulation of TG distribution, trafficking, and turnover in enterocytes (Khaldoun et al., 2014; Narabayashi et al., 2015). Therefore, it is reasonable to propose that RACK1 is involved in these processes. Future studies are required to address these issues.

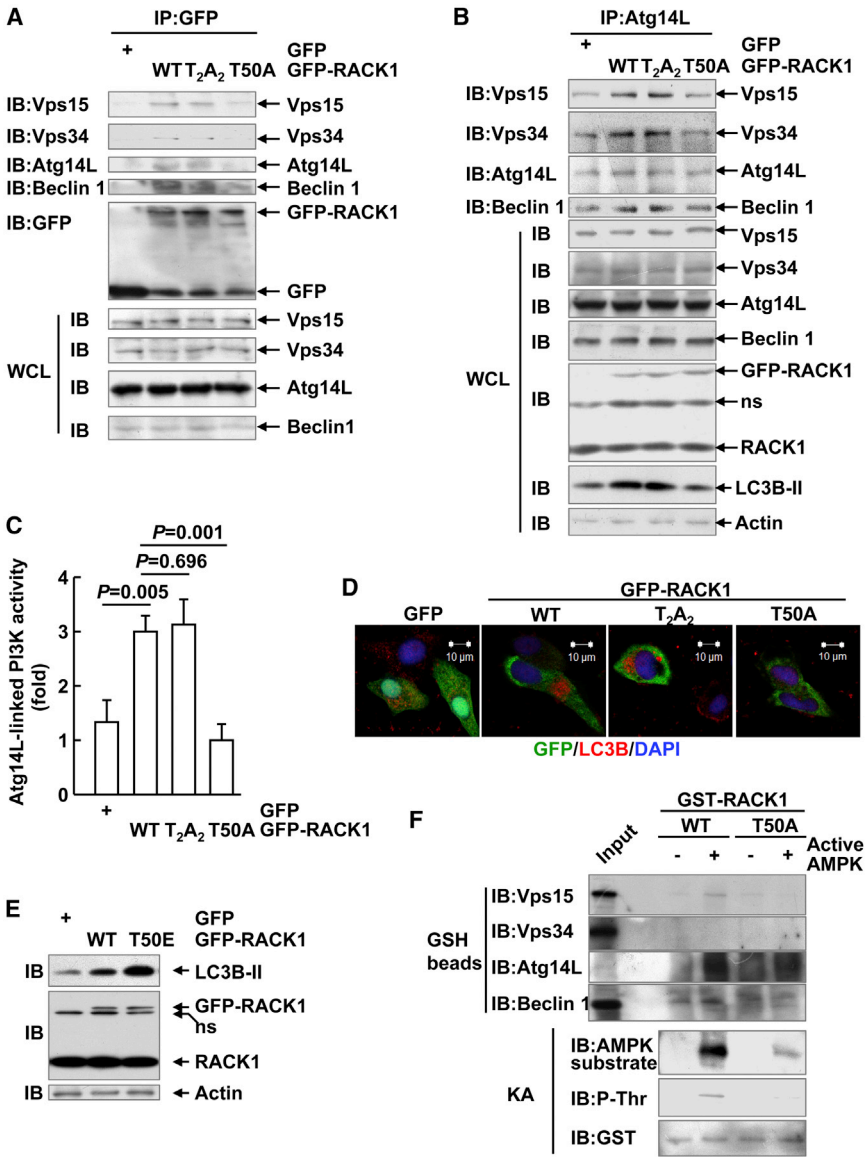

Figure 7. Thr50 Phosphorylation of RACK1 Promotes Its Direct Binding to Atg14L, Beclin 1, and Vps15

HepG2 cells with stable RACK1 knockdown were transfected with mammalian expression vectors encoding GFP-tagged shRNA-resistant RACK1 WT and mutants.

(A–E) In (A), (B), and (E), cell lysates were subjected to immunoprecipitation with the indicated antibodies. Precipitates were then subjected to SDS-PAGE and IB with the indicated antibodies. ns, nonspecific. Note that LC3B-I was not detected. WCL, whole-cell lysates. (C) Cell lysates were subjected to immunoprecipitation with an antibody against Atg14L and Atg14L-linked Vps34 kinase activity was measured with the Class III PI3K ELISA Kit. (D) Cells were subjected to indirect IF analysis of endogenous LC3B.

(F) GST-RACK1 WT and GST-RACK1 T50A, before or after in vitro phosphorylation by active AMPK complex, were incubated with GSH beads and mixed with the in-vitro-translated GFP-Atg14L, Beclin 1, Myc-Vps34, and His-Vps15. Precipitates were subjected to SDS-PAGE and IB with the indicated antibodies.

Emerging evidence suggests that scaffold proteins Dapper1, NRBF2, and Atg38 are indispensable for the formation of the autophagy-initiation complex upon starvation (Araki et al., 2013; Lu et al., 2014; Ma et al., 2014). Interestingly, ablation of Dapper1, NRBF2, or Atg38 shows marginal effects on basal autophagy (Araki et al., 2013; Lu et al., 2014; Ma et al., 2014). By contrast, ablation RACK1 leads to impaired autophagy at the basal state as well as upon starvation. Thus, it is possible that the assembly of the autophagy-initiation complex at the basal state largely depends on RACK1, whereas, upon starvation, various scaffold proteins contribute to its assembly. In line with this notion, the liver damage in *Gnb2l1*$^{\Delta hep}$ mice is relatively mild compared with that in *Atg5*$^{\Delta hep}$, *Atg7*$^{\Delta hep}$, and *Vps34*$^{-/-}$ mice (Jaber et al., 2012; Komatsu et al., 2005; Singh et al., 2009; Takamura et al., 2011) but is much more evident than that in NRBF2-deficient mice (Lu et al., 2014). Consequently, the liver damage associated with lipid accumulation in *Gnb2l1*$^{\Delta hep}$ mice eventually leads to spontaneous tumors (Figures S1C and S1D), similar to mice with systemic mosaic deletion of Atg5 and *Atg7*$^{\Delta hep}$ mice that develop benign liver adenomas (Takamura et al., 2011). Moreover, RACK1 deficiency resulted in the augmented secretion of IL-1β from peritoneal macrophages (Figure S2E), consistent with the previous reports that defective autophagy enhances endotoxin-induced IL-1β production (Nakahira et al., 2011; Saitoh et al., 2008). The aforementioned facts confirm the essential engagement of RACK1 in autophagy. Despite that, we failed to see typical punctuate structure of RACK1 at the basal state and upon classical starvation in cells of liver origin (data not shown). Possibly, this is because RACK1 is highly expressed in this type of cell, and only a small portion of RACK1 is involved in autophagy onset.

It is important to identify the AMPK substrate(s) involved in autophagy. Besides directly phosphorylating and activating Ulk1, AMPK also phosphorylates TSC2 and Raptor, key regulators of mTOR, thereby inhibiting the suppressive effect of mTOR (Egan et al., 2011; Kim et al., 2011). Here, we report that RACK1 is a substrate of AMPK. AMPK phosphorylates RACK1 at Thr50, which facilitates the direct binding of RACK1 to Vps15, Atg14L, and Beclin 1. Consequently, RACK1 participates in the formation of autophagosome biogenesis complex. Because both LPS-induced autophagy and basal autophagy were suppressed upon RACK1 knockdown (Figure 2F), our data imply that treatment of LPS induces the phosphorylation of RACK1

through AMPK and that the subpopulation of RACK1 is phosphorylated by AMPK even in non-starved conditions. Indeed, transforming growth factor β (TGFβ)-activated kinase 1 (TAK1), a kinase strongly activated by LPS, has been reported to activate AMPK and contributes to autophagy induction (Herrero-Martín et al., 2009). These findings lead to the notion that the autophagy machinary pushes adaptors into the autophagy-initiating complex. The corresponding upstream signals for Dapper1, NRBF2, or Atg38 remain to be explored.

EXPERIMENTAL PROCEDURES

Mice

Mice were generated at the Shanghai Research Center for Biomodel Organisms. Frt-flanked neomycin cassette was introduced in the region between exon 1 and exon 2 of the *Gnb2l1* gene. *LoxP* sites were situated surrounding exon 2 and after the Frt-Neo-Frt sequence (Figure S1A). The construct was electroporated into 129/SvEv embryonic stem (ES) cells. After neomycin selection, the ES cells were injected into the foster mothers of C57 BL/6J background to create chimeric mice that transmitted the mutated *Gnb2l1* allele through the germline. The mice were backcrossed to the C57 BL/6J strain (Jackson Laboratory). Mice homozygous for a *Gnb2l1* conditional allele ($Gnb2l1^{F/F}$) were crossed with mice (Jackson Laboratory) expressing a transgene encoding *Cre* recombinase driven by the *Albumin* promoter and enhancer (*Alb-Cre* mice) or under the control of α/β-interferon-inducible Mx promoter (*Mx-Cre* mice). Cre recombinase activity was initiated by intraperitoneal injection of poly(I:C) (InvivoGen) at the dose of 5 μg/g every 2 days for a total of three injections, which induces α/β-interferon production. $Gnb2l1^{F/F;\ Alb\text{-}Cre}$ (named as $Gnb2l1^{\Delta hep}$) or $Gnb2l1^{F/F;\ Mx\text{-}Cre}$ mice were kept in the animal facility of the Institute of Biotechnology (20 Dongdajie, Beijing 100071, PRC). The genotypes were determined by PCR of tissue-extracted DNA (Figure S1B). PCR primers for the *Gnb2l1* conditional allele were: 5′-CGCTGCGCCTCTGGGATCTCA-3′ (forward) and 5′-TGGTGTGGCCGA CAAATCGCC-3′ (reverse). Animals were handled in accordance with the guidelines of the Institute of Basic Medical Sciences. Littermate controls ($Gnb2l1^{F/F}$) were used in all experiments.

Cell Culture, Transfection, and Transduction

The two-step collagenase perfusion technique was used for the isolation of large numbers of viable adult hepatocytes (Klaunig et al., 1981). Cell lines were purchased from the Shanghai Institutes for Biological Sciences. All cells were cultured in DMEM supplemented with 10% fetal bovine serum, 100 U/ml penicillin, and 100 μg/ml streptomycin and were maintained at 37°C with 5% carbon dioxide. HepG2 cells stably expressing RACK1 shRNA or NC shRNA have been described previously (Guo et al., 2013). Transfection was performed with Lipofectamine 2000 (Invitrogen). Transduction was performed with lentivirus (MOI = 10).

IF

IF was performed as previously described (Cui et al., 2009).

Co-IP and IB

Co-IP and IB were performed as previously described (Wang et al., 2010; Zhang et al., 2008, 2010). Liver tissues were dissected and homogenized in RIPA buffer (50 mM Tris-HCl, pH 7.5, 1% NP-40, 0.35% deoxycholate, 150 mM NaCl, 1 mM EDTA, 1 mM EGTA, supplemented with protease and phosphatase inhibitor cocktails) or IP lysis buffer (10 mM Tris-HCl, pH 7.5, 2 mM EDTA, 1% NP-40, 150 mM NaCl, supplemented with protease and phosphatase inhibitor cocktail). To identify the bound proteins and the phosphorylation of endogenous-like GFP-RACK1, anti-GFP immunoprecipitates were subjected to SDS-PAGE. After silver staining (Invitrogen), specific protein bands were cut, in-gel digested, and subjected to nano-liquid chromatography (nano-LC)-MS/MS analysis at the National Center of Biomedical Analysis (Beijing, PRC) Mass Spectrometry facility. The resulting peaklist was subjected to database searching using the Mascot search engine.

Statistics

Results are shown as mean ± SD. Differences were considered significant with a p value < 0.05 using Student's t test (paired or unpaired) and one-way ANOVA.

SUPPLEMENTAL INFORMATION

Supplemental Information includes Supplemental Experimental Procedures, seven figures, and one table and can be found with this article online at http://dx.doi.org/10.1016/j.celrep.2015.10.011.

AUTHOR CONTRIBUTIONS

J.Z. conceived and designed the study, analyzed the data, and wrote the paper, Y.Z. performed almost all the cell biology experiments. Z.J. finished a few cell biology experiments. Q.W. did all the animal experiments. G.Q. made the constructs. S.Z. and J.W. performed genotyping. Y.C. provided key reagents. W.W. generated the stable clones. J.C., K.H., and Q.C. performed flow cytometry. B.S. and Y.M. performed statistical analysis. W.J.Z. provided *Alb-Cre* mice.

ACKNOWLEDGMENTS

We thank Profs. Zhigang Tian and Rui Sun (University of Science and Technology of China) for helpful discussion and technical guidance. This work was supported by grants from the National Natural Science Foundation of China (81472736 and 31270960 to J.Z.).

Received: April 2, 2015
Revised: September 7, 2015
Accepted: October 2, 2015
Published: November 5, 2015

REFERENCES

Araki, Y., Ku, W.C., Akioka, M., May, A.I., Hayashi, Y., Arisaka, F., Ishihama, Y., and Ohsumi, Y. (2013). Atg38 is required for autophagy-specific phosphatidylinositol 3-kinase complex integrity. J. Cell Biol. *203*, 299–313.

Axe, E.L., Walker, S.A., Manifava, M., Chandra, P., Roderick, H.L., Habermann, A., Griffiths, G., and Ktistakis, N.T. (2008). Autophagosome formation from membrane compartments enriched in phosphatidylinositol 3-phosphate and dynamically connected to the endoplasmic reticulum. J. Cell Biol. *182*, 685–701.

Belozerov, V.E., Ratkovic, S., McNeill, H., Hilliker, A.J., and McDermott, J.C. (2014). *In vivo* interaction proteomics reveal a novel p38 mitogen-activated protein kinase/Rack1 pathway regulating proteostasis in *Drosophila* muscle. Mol. Cell. Biol. *34*, 474–484.

Bhutia, S.K., Kegelman, T.P., Das, S.K., Azab, B., Su, Z.Z., Lee, S.G., Sarkar, D., and Fisher, P.B. (2010). Astrocyte elevated gene-1 induces protective autophagy. Proc. Natl. Acad. Sci. USA *107*, 22243–22248.

Chang, B.Y., Harte, R.A., and Cartwright, C.A. (2002). RACK1: a novel substrate for the Src protein-tyrosine kinase. Oncogene *21*, 7619–7629.

Chu, C.T., Zhu, J., and Dagda, R. (2007). Beclin 1-independent pathway of damage-induced mitophagy and autophagic stress: implications for neurodegeneration and cell death. Autophagy *3*, 663–666.

Cui, J., Wang, Q., Wang, J., Lv, M., Zhu, N., Li, Y., Feng, J., Shen, B., and Zhang, J. (2009). Basal c-Jun NH2-terminal protein kinase activity is essential for survival and proliferation of T-cell acute lymphoblastic leukemia cells. Mol. Cancer Ther. *8*, 3214–3222.

Egan, D.F., Shackelford, D.B., Mihaylova, M.M., Gelino, S., Kohnz, R.A., Mair, W., Vasquez, D.S., Joshi, A., Gwinn, D.M., Taylor, R., et al. (2011). Phosphorylation of ULK1 (hATG1) by AMP-activated protein kinase connects energy sensing to mitophagy. Science *331*, 456–461.

Erdi, B., Nagy, P., Zvara, A., Varga, A., Pircs, K., Ménesi, D., Puskás, L.G., and Juhász, G. (2012). Loss of the starvation-induced gene Rack1 leads to glycogen deficiency and impaired autophagic responses in Drosophila. Autophagy *8*, 1124–1135.

Guo, Y., Wang, W., Wang, J., Feng, J., Wang, Q., Jin, J., Lv, M., Li, X., Li, Y., Ma, Y., et al. (2013). Receptor for activated C kinase 1 promotes hepatocellular carcinoma growth by enhancing mitogen-activated protein kinase kinase 7 activity. Hepatology *57*, 140–151.

Hara, T., Nakamura, K., Matsui, M., Yamamoto, A., Nakahara, Y., Suzuki-Migishima, R., Yokoyama, M., Mishima, K., Saito, I., Okano, H., and Mizushima, N. (2006). Suppression of basal autophagy in neural cells causes neurodegenerative disease in mice. Nature *441*, 885–889.

Herrero-Martín, G., Høyer-Hansen, M., García-García, C., Fumarola, C., Farkas, T., López-Rivas, A., and Jäättelä, M. (2009). TAK1 activates AMPK-dependent cytoprotective autophagy in TRAIL-treated epithelial cells. EMBO J. *28*, 677–685.

Itakura, E., and Mizushima, N. (2010). Characterization of autophagosome formation site by a hierarchical analysis of mammalian Atg proteins. Autophagy *6*, 764–776.

Jaber, N., Dou, Z., Chen, J.S., Catanzaro, J., Jiang, Y.P., Ballou, L.M., Selinger, E., Ouyang, X., Lin, R.Z., Zhang, J., and Zong, W.X. (2012). Class III PI3K Vps34 plays an essential role in autophagy and in heart and liver function. Proc. Natl. Acad. Sci. USA *109*, 2003–2008.

Khaldoun, S.A., Emond-Boisjoly, M.A., Chateau, D., Carrière, V., Lacasa, M., Rousset, M., Demignot, S., and Morel, E. (2014). Autophagosomes contribute to intracellular lipid distribution in enterocytes. Mol. Biol. Cell *25*, 118–132.

Kiely, P.A., Baillie, G.S., Barrett, R., Buckley, D.A., Adams, D.R., Houslay, M.D., and O'Connor, R. (2009). Phosphorylation of RACK1 on tyrosine 52 by c-Abl is required for insulin-like growth factor I-mediated regulation of focal adhesion kinase. J. Biol. Chem. *284*, 20263–20274.

Kim, K.H., and Lee, M.S. (2014). Autophagy—a key player in cellular and body metabolism. Nat. Rev. Endocrinol. *10*, 322–337.

Kim, J., Kundu, M., Viollet, B., and Guan, K.L. (2011). AMPK and mTOR regulate autophagy through direct phosphorylation of Ulk1. Nat. Cell Biol. *13*, 132–141.

Klaunig, J.E., Goldblatt, P.J., Hinton, D.E., Lipsky, M.M., Chacko, J., and Trump, B.F. (1981). Mouse liver cell culture. I. Hepatocyte isolation. In Vitro *17*, 913–925.

Komatsu, M., Waguri, S., Ueno, T., Iwata, J., Murata, S., Tanida, I., Ezaki, J., Mizushima, N., Ohsumi, Y., Uchiyama, Y., et al. (2005). Impairment of starvation-induced and constitutive autophagy in *Atg7*-deficient mice. J. Cell Biol. *169*, 425–434.

Kraft, C., and Martens, S. (2012). Mechanisms and regulation of autophagosome formation. Curr. Opin. Cell Biol. *24*, 496–501.

Li, A.C., and Glass, C.K. (2002). The macrophage foam cell as a target for therapeutic intervention. Nat. Med. *8*, 1235–1242.

Liang, C., Feng, P., Ku, B., Dotan, I., Canaani, D., Oh, B.H., and Jung, J.U. (2006). Autophagic and tumour suppressor activity of a novel Beclin1-binding protein UVRAG. Nat. Cell Biol. *8*, 688–699.

Liu, C.L., Yu, I.S., Pan, H.W., Lin, S.W., and Hsu, H.C. (2007). L2dtl is essential for cell survival and nuclear division in early mouse embryonic development. J. Biol. Chem. *282*, 1109–1118.

Lu, J., He, L., Behrends, C., Araki, M., Araki, K., Wang, Q.J., Catanzaro, J.M., Friedman, S.L., Zong, W.X., Fiel, M.I., et al. (2014). NRBF2 regulates autophagy and prevents liver injury by modulating Atg14L-linked phosphatidylinositol-3 kinase III activity. Nat. Commun. *5*, 3920.

Ma, B., Cao, W., Li, W., Gao, C., Qi, Z., Zhao, Y., Du, J., Xue, H., Peng, J., Wen, J., et al. (2014). Dapper1 promotes autophagy by enhancing the Beclin1-Vps34-Atg14L complex formation. Cell Res. *24*, 912–924.

Matsunaga, K., Saitoh, T., Tabata, K., Omori, H., Satoh, T., Kurotori, N., Maejima, I., Shirahama-Noda, K., Ichimura, T., Isobe, T., et al. (2009). Two Beclin 1-binding proteins, Atg14L and Rubicon, reciprocally regulate autophagy at different stages. Nat. Cell Biol. *11*, 385–396.

McCue, M.D. (2010). Starvation physiology: reviewing the different strategies animals use to survive a common challenge. Comp. Biochem. Physiol. A Mol. Integr. Physiol. *156*, 1–18.

Mizushima, N., and Komatsu, M. (2011). Autophagy: renovation of cells and tissues. Cell *147*, 728–741.

Nakahira, K., Haspel, J.A., Rathinam, V.A., Lee, S.J., Dolinay, T., Lam, H.C., Englert, J.A., Rabinovitch, M., Cernadas, M., Kim, H.P., et al. (2011). Autophagy proteins regulate innate immune responses by inhibiting the release of mitochondrial DNA mediated by the NALP3 inflammasome. Nat. Immunol. *12*, 222–230.

Nakai, A., Yamaguchi, O., Takeda, T., Higuchi, Y., Hikoso, S., Taniike, M., Omiya, S., Mizote, I., Matsumura, Y., Asahi, M., et al. (2007). The role of autophagy in cardiomyocytes in the basal state and in response to hemodynamic stress. Nat. Med. *13*, 619–624.

Narabayashi, K., Ito, Y., Eid, N., Maemura, K., Inoue, T., Takeuchi, T., Otsuki, Y., and Higuchi, K. (2015). Indomethacin suppresses LAMP-2 expression and induces lipophagy and lipoapoptosis in rat enterocytes via the ER stress pathway. J. Gastroenterol. *50*, 541–554.

Postic, C., Shiota, M., Niswender, K.D., Jetton, T.L., Chen, Y., Moates, J.M., Shelton, K.D., Lindner, J., Cherrington, A.D., and Magnuson, M.A. (1999). Dual roles for glucokinase in glucose homeostasis as determined by liver and pancreatic beta cell-specific gene knock-outs using Cre recombinase. J. Biol. Chem. *274*, 305–315.

Razani, B., Feng, C., Coleman, T., Emanuel, R., Wen, H., Hwang, S., Ting, J.P., Virgin, H.W., Kastan, M.B., and Semenkovich, C.F. (2012). Autophagy links inflammasomes to atherosclerotic progression. Cell Metab. *15*, 534–544.

Ruan, Y., Sun, L., Hao, Y., Wang, L., Xu, J., Zhang, W., Xie, J., Guo, L., Zhou, L., Yun, X., et al. (2012). Ribosomal RACK1 promotes chemoresistance and growth in human hepatocellular carcinoma. J. Clin. Invest. *122*, 2554–2566.

Russell, R.C., Tian, Y., Yuan, H., Park, H.W., Chang, Y.Y., Kim, J., Kim, H., Neufeld, T.P., Dillin, A., and Guan, K.L. (2013). ULK1 induces autophagy by phosphorylating Beclin-1 and activating VPS34 lipid kinase. Nat. Cell Biol. *15*, 741–750.

Saitoh, T., Fujita, N., Jang, M.H., Uematsu, S., Yang, B.G., Satoh, T., Omori, H., Noda, T., Yamamoto, N., Komatsu, M., et al. (2008). Loss of the autophagy protein Atg16L1 enhances endotoxin-induced IL-1beta production. Nature *456*, 264–268.

Singh, R., Kaushik, S., Wang, Y., Xiang, Y., Novak, I., Komatsu, M., Tanaka, K., Cuervo, A.M., and Czaja, M.J. (2009). Autophagy regulates lipid metabolism. Nature *458*, 1131–1135.

Stirnimann, C.U., Petsalaki, E., Russell, R.B., and Müller, C.W. (2010). WD40 proteins propel cellular networks. Trends Biochem. Sci. *35*, 565–574.

Takamura, A., Komatsu, M., Hara, T., Sakamoto, A., Kishi, C., Waguri, S., Eishi, Y., Hino, O., Tanaka, K., and Mizushima, N. (2011). Autophagy-deficient mice develop multiple liver tumors. Genes Dev. *25*, 795–800.

Urano, D., Czarnecki, O., Wang, X., Jones, A.M., and Chen, J.G. (2015). Arabidopsis receptor of activated C kinase1 phosphorylation by WITH NO LYSINE8 KINASE. Plant Physiol. *167*, 507–516.

Wang, J., Tang, R., Lv, M., Zhang, J., and Shen, B. (2010). Selective unresponsiveness to the inhibition of p38 MAPK activation by cAMP helps L929 fibroblastoma cells escape TNF-α-induced cell death. Mol. Cancer *9*, 6.

Wei, Y., Pattingre, S., Sinha, S., Bassik, M., and Levine, B. (2008). JNK1-mediated phosphorylation of Bcl-2 regulates starvation-induced autophagy. Mol. Cell *30*, 678–688.

Zhang, J., Wang, Q., Zhu, N., Yu, M., Shen, B., Xiang, J., and Lin, A. (2008). Cyclic AMP inhibits JNK activation by CREB-mediated induction of c-FLIP($_L$) and MKP-1, thereby antagonizing UV-induced apoptosis. Cell Death Differ. *15*, 1654–1662.

Zhang, J., Zhu, N., Wang, Q., Wang, J., Ma, Y., Qiao, C., Li, Y., Li, X., Su, B., and Shen, B. (2010). MEKK3 overexpression contributes to the hyperresponsiveness of IL-12-overproducing cells and CD4+ T conventional cells in non-obese diabetic mice. J. Immunol. *185*, 3554–3563.

Zoncu, R., Efeyan, A., and Sabatini, D.M. (2011). mTOR: from growth signal integration to cancer, diabetes and ageing. Nat. Rev. Mol. Cell Biol. *12*, 21–35.